

Ring Expansion of a Platinacyclopropane to a Platinacyclopentane by Double Insertion of Isocyanides into Pt–C Bonds

Kazuhiro Tsuchiya, Hideo Kondo, and Hideo Nagashima*

Graduate School of Engineering Sciences, and Institute for Materials Chemistry and Engineering, Kyushu University, Kasuga, Fukuoka 816-8580, Japan

Received September 23, 2006

A platinum isocyanide complex bearing a η^2 -TCNE ligand, $(\eta^2\text{-TCNE})\text{Pt}(\eta\text{-CNC}_6\text{H}_3\text{-2,6-Me}_2)_2$ (**1**), was synthesized, and its crystallographic study revealed the coordination mode of the η^2 -TCNE ligand to be a typical metallacyclopropane extreme, in which back-donation from metal to TCNE contributes primarily to the stabilization of **1**. Treatment of **1** with 2 equiv of $\text{CNC}_6\text{H}_3\text{-2,6-Me}_2$ resulted in ring expansion of the platinacyclopropane by insertion of $\text{CNC}_6\text{H}_3\text{-2,6-Me}_2$ into each Pt–C bond of the metallacycle, leading to formation of a new complex having a platinacyclopentane structure, $(\text{TCNE})\text{-Pt}(\eta\text{-CNC}_6\text{H}_3\text{-2,6-Me}_2)_4$ (**4**). Although the molecular structures of palladium and nickel homologues of **1** were close to the corresponding metallacyclopropane, no metallacyclopentane complex was obtained under similar conditions. Studies on variable-temperature NMR spectroscopy and spin-saturation transfer measurement of **4** showed exchange of the imidoyl $\text{CNC}_6\text{H}_3\text{-2,6-Me}_2$ group and the coordinated $\text{CNC}_6\text{H}_3\text{-2,6-Me}_2$ ligand in solution, suggesting the ring expansion to be reversible.

Introduction

It is well known that coordination of alkenes to transition metal is qualitatively explained by the Dewar–Chatt–Duncanson model,¹ in which the metal–ligand interaction is established by the balance of two electronic factors, donation of π -electrons from bonding orbitals of alkene to unoccupied metal orbitals and back-donation of d-electrons from occupied metal orbitals to antibonding orbitals of alkene.^{2–6} As shown in Figure 1, two extreme cases have been discussed in organometallic chemistry; combination of strong donation with weak back-donation provides a “ π -complex extreme”, whereas the reverse case, i.e., larger contribution of back-donation than that of donation affords a “metallacyclopropane extreme”. In platinum–alkene complexes, Zeise’s salt, $\text{K}[(\text{C}_2\text{H}_4)\text{PtCl}_3]\cdot\text{H}_2\text{O}$, is a representative of a “ π -complex extreme”; interaction of the HOMO of ethylene

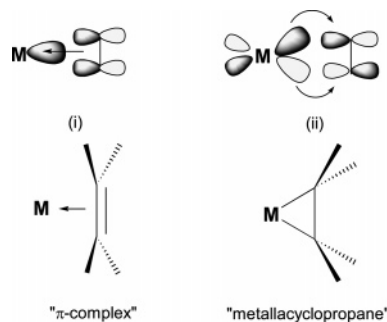


Figure 1. Components of transition metal–olefin interaction [(i) σ -donation, (ii) π -back-donation].

with unoccupied orbitals of a weakly π -basic Pt(II) fragment makes the carbon–carbon bond distance [$1.345(4)$ Å]⁷ slightly longer than that of uncoordinated ethylene [$1.337(2)$ Å],⁸ while the planarity of ethylene remains intact. In sharp contrast, $(\eta^2\text{-TCNE})\text{Pt}(\kappa\text{-PPh}_3)_2$ is well recognized as a typical example of a “metallacyclopropane extreme”; interaction of occupied orbitals of Pt(0) with the LUMO of ethylene contributes to significant elongation of the carbon–carbon bond length [TCNE bound to $\text{Pt}(\kappa\text{-PPh}_3)_2$; $\text{C}=\text{C}$ 1.494 Å; uncoordinated TCNE; $\text{C}=\text{C}$ 1.344–(3) Å]^{9,10} and change of the hybridization of the olefinic carbons of TCNE from sp^2 to sp^3 on coordination.

The structure and the electronic structure of the “ π -complex extreme” and “metallacyclopropane extreme” are sometimes discussed in terms of mechanisms of several organometallic reactions.^{11–14} Reaction of nucleophiles with the coordinated alkene may be related to the “ π -complex extreme”, in which the electron donation of π -electrons of alkenes to the metal

* Corresponding author. E-mail: nagasima@cm.kyushu-u.ac.jp.

(1) (a) Dewar, M. J. S. *Bull. Soc. Chim. Fr.* **1951**, 18, C79. (b) Chatt, J.; Duncanson, L. A. *J. Chem. Soc.* **1953**, 2939.

(2) (a) Crabtree, R. H., Ed. *The Organometallic Chemistry of the Transition Metals*, 4th ed.; Wiley: New York, 2001; Chapter 3, p 125. (b) Ittel, S. D.; Ibers, J. A. *Adv. Organomet. Chem.* **1976**, 14, 33. (c) Collman, J. P.; Hegedus, L. S. *Principles and Applications of Organotransition Metal Chemistry*, 2nd ed.; University Science Books: Mill Valley, CA, 1987; Chapter 3, p 149. (d) Elschenbroich C.; Salzer, A. *Organometallics*, 2nd ed.; VCH: Weinheim, 1992; Chapter 15, p 252.

(3) (a) Wunderlich, J. A.; Mellor, D. P. *Acta Crystallogr.* **1954**, 7, 130. (b) Jarvis, J. A. J.; Kilbourn, B. T.; Owston, P. G. *Acta Crystallogr.* **1971**, B27, 366.

(4) (a) Panattoni, C.; Bombieri, G.; Belluco, U.; Baddley, W. H. *J. Am. Chem. Soc.* **1968**, 90, 798. (b) Bombieri, G.; Forsellini, E.; Panattoni, C.; Graziani, R.; Bandoli, G. *J. Chem. Soc. A* **1970**, 1313.

(5) (a) Thorn, M. G.; Hill, J. E.; Waratuke, S. A.; Johnson, E. S.; Fanwick, P. E.; Rothwell, I. P. *J. Am. Chem. Soc.* **1997**, 119, 8630. (b) Curnow, O. J.; Huges, R. P.; Mairs, E. N.; Reingold, A. L. *Organometallics* **1993**, 12, 3102. (c) van Asselt, R.; Elsevier, C. J.; Smeets, W. J. J.; Spek, A. L. *Inorg. Chem.* **1994**, 33, 1521.

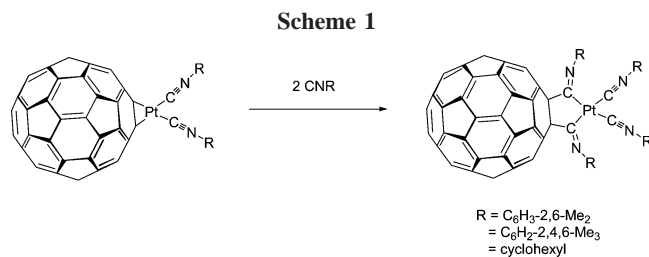
(6) For a review: (a) Frenking, G.; Fröhlich, N. *Chem. Rev.* **2000**, 100, 717, and reference therein. Typical examples, see: (b) Åkermark, B.; Almemark, M.; Almlöf, J.; Bäckvall, J.-E.; Roos, B.; Størd, Å. *J. Am. Chem. Soc.* **1977**, 99, 4617. (c) Albright, T. A.; Hoffmann, R.; Thibeault, J. C.; Thorn, D. L. *J. Am. Chem. Soc.* **1979**, 101, 3801. (d) Rösch, N.; Messner, R. P.; Johnson, K. H. *J. Am. Chem. Soc.* **1974**, 96, 3855. (e) Ziegler, T.; Rauk, A. *Inorg. Chem.* **1979**, 18, 1558.

(7) Love, R. A.; Koetzle, T. F.; Williams, G. J. B.; Andrews, L. C.; Bau, R. *Inorg. Chem.* **1975**, 11, 2653.

(8) Bartell, L. S.; Roth, E. A.; Hollowell, C. D.; Kuchitsu, K.; Young, J. E., Jr. *J. Chem. Phys.* **1965**, 42, 2683.

(9) Bombieri, G.; Forsellini, E.; Panattoni, C.; Graziani, R.; Bandoli, G. *J. Chem. Soc. A* **1970**, 8, 1313.

(10) (a) Little, R. G.; Pautler, D.; Coppens, P. *Acta Crystallogr., Sect. B* **1971**, 27, 1493. (b) Hope, H. *Acta Chem. Scand.* **1968**, 22, 1057.



center increases the cationic nature of the carbon of the coordinated alkenes; this facilitates the reaction with nucleophiles.¹³ In contrast, the “metallacyclopropane extreme” is considered to be a strained three-membered ring structure consisting of two metal–carbon bonds and one carbon–carbon single bond; insertion of alkenes into the metal–carbon bond results in ring expansion to the metallacyclopentane. This reaction is often used in the mechanisms of catalytic oxidative cycloaddition reactions of alkenes.¹⁴

Although the chemistry of the “platinacyclopropane extreme” is one of the well-investigated issues in organometallic chemistry,^{4,9,15} little has been discussed on the possibility of insertion of unsaturated molecules into the Pt–C bond. Thus, the starting point of this paper is the question of whether the platinum–alkene complexes having a “platinacyclopropane extreme” structure, which is unequivocally determined, undergo the insertion of unsaturated molecules into the platinum–carbon bonds leading to the ring expansion reactions. A clue to solve this question is already available from our earlier studies on the metal complexes of fullerenes; we obtained spectroscopic evidence suggesting that $(\eta^2\text{-C}_{60})\text{Pt}(\eta\text{-CNR})_2$ reacts with 2 equiv of CNR to form a novel platinum complex having a platinacyclopentane structure (Scheme 1).¹⁶ Since C_{60} is a strong electron acceptor, $(\eta^2\text{-C}_{60})\text{Pt}(\eta\text{-CNR})_2$ is expected to have a structure close to the platinacyclopropane extreme having two Pt–C bonds. Insertion of CNR into each Pt–C bond results in ring expansion to the platinacyclopentane. Since closely related

(11) (a) Steigerwald, M. L.; Goddard, W. A., III. *J. Am. Chem. Soc.* **1985**, *107*, 5027. (b) Oxgaard, J.; Periana, R. A.; Goddard, W. A., III. *J. Am. Chem. Soc.* **2004**, *126*, 11658.

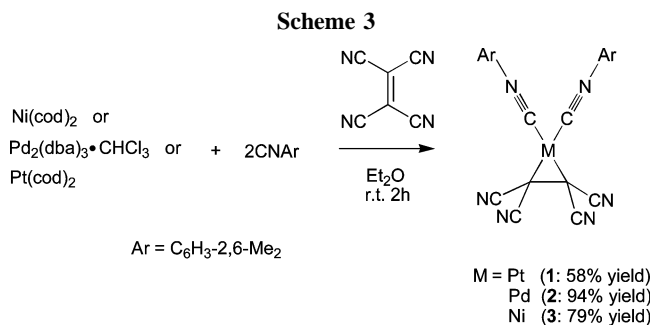
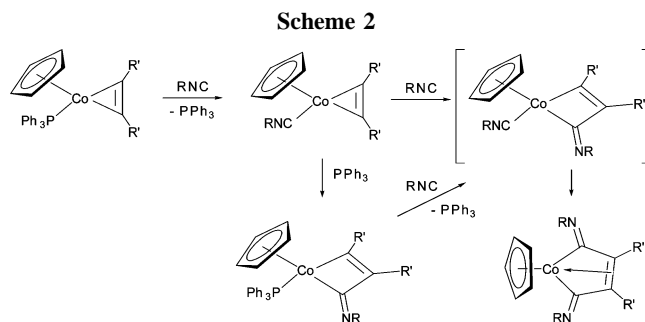
(12) Baddley, W. H. *Inorg. Chem. Acta* **1968**, *7*.

(13) (a) McDaniel, K. F. In *Comprehensive Organometallic Chemistry II*; Abel, E. W., Stone, F. G. A., Wilkinson, G., Eds.; Elsevier: New York, 1995; Vol. 12, p 601. (b) Maitlis, P. M. *The Organic Chemistry of Palladium*; Academic Press: New York, 1971; Vol. 2, p 7. (c) Smidt, J.; Hafner, W.; Jira, R.; Sieber, R.; Sedlmeier, J.; Sable, A. *Angew. Chem., Int. Ed. Engl.* **1962**, *1*, 80. (d) Palumbo, R.; de Renzi, A.; Panunzi, A.; Paiaro, G. *J. Am. Chem. Soc.* **1969**, *91*, 3874. (e) Åkermark, B.; Bäckvall, J.-E.; Hegedus, L. S.; Siirala-Hansen, K.; Sjöberg, K.; Zetterberg, K. *J. Organomet. Chem.* **1974**, *72*, 127.

(14) (a) Schrock, R. R.; McLain, S.; Sancho, J. *Pure Appl. Chem.* **1980**, *52*, 729. (b) Erker, G.; Kropp, K. *J. Am. Chem. Soc.* **1979**, *101*, 3659. (c) McAlister, D. R.; Erwin, D. K.; Bercaw, J. E. *J. Am. Chem. Soc.* **1978**, *100*, 5966. (d) Fraser, A. P.; Bird, P. H.; Bezman, S. A.; Shapley, J. R.; White, R.; Osborn, J. A. *J. Am. Chem. Soc.* **1973**, *95*, 597. (e) McDermott, J. X.; Wilson, M. E.; Whitesides, G. M. *J. Am. Chem. Soc.* **1976**, *98*, 6529. (f) Maitlis, P. M. *The Organic Chemistry of Palladium*; Academic Press: New York, 1971; Vol. 2, p 32. (g) Mango, F. D.; Schachtschneider, J. H. *J. Am. Chem. Soc.* **1967**, *89*, 2484. (h) Mango, F. D. *Tetrahedron Lett.* **1971**, 505.

(15) (a) Song, L.-C.; Liu, P.-C.; Liu, J.-T.; Su, F.-H.; Wang, G.-F.; Hu, Q.-M.; Zanello, P.; Laschi, F.; Fontani, M. *Eur. J. Inorg. Chem.* **2003**, 3201. (b) Phillips, I. G.; Ball, R. G.; Cavell, R. G. *Inorg. Chem.* **1987**, *26*, 4074. (c) Nicolaides, A.; Smith, J. M.; Kumar, A.; Barnhart, D. M.; Borden, W. T. *Organometallics* **1995**, *14*, 3475. (d) da Silva, M. F. C. G.; da Silva, J. J. R. F.; Pombeiro, A. J. L.; Bertani, R.; Michelin, R. A.; Mozzon, M.; Benetollo, F.; Bombieri, G. *Inorg. Chem. Acta* **1993**, *214*, 85. (e) Francis, J. N.; McAdam, A.; Ibers, J. A. *J. Organomet. Chem.* **1971**, *29*, 131. (f) Osborne, R. B.; Lewis, H. C.; Ibers, J. A. *J. Organomet. Chem.* **1981**, *208*, 125.

(16) Nagashima, H.; Nakazawa, M.; Furukawa, T.; Itoh, K. *Chem. Lett.* **1996**, *5*, 405.



double insertion of isocyanides to a η^2 -alkyne–cobalt complex was reported by Yamazaki and Wakatsuki in 1975,¹⁷ in which reaction of two CNR is considered to give ring expansion of the cobaltacyclopropene complex to the compound having a cobaltacyclopentene structure (Scheme 2), the ring expansion from platinacyclopropane to platinacyclopentane by double insertion of CNR into $(\eta^2\text{-C}_{60})\text{Pt}(\eta\text{-CNR})_2$ seemed to be reasonable. However, lack of crystallographic evidence proving the platinacyclopropane structure of $(\eta^2\text{-C}_{60})\text{Pt}(\eta\text{-CNR})_2$ and the platinacyclopentane structure of the double-insertion product was a problem for further investigation on the ring expansion reaction. In this paper, we report a solution to this problem using TCNE instead of C_{60} . Ring expansion of $(\eta^2\text{-TCNE})\text{Pt}(\eta\text{-CNC}_6\text{H}_3\text{-2,6-Me}_2)_2$ (**1**), having a platinacyclopropane structure, to the platinacyclopentane **4** takes place by double insertion of $\text{CNC}_6\text{H}_3\text{-2,6-Me}_2$ into the Pt–C bonds of **1**, which was unequivocally evidenced by spectroscopic and crystallographic studies. Preparation and reactions of nickel and palladium homologues of **1** and the exchange process of $\eta\text{-C}\equiv\text{NC}_6\text{H}_3\text{-2,6-Me}_2$ and $\eta\text{-C}\equiv\text{NC}_6\text{H}_3\text{-2,6-Me}_2$ units in the platinacyclopentane contribute to understanding the mechanisms of the ring expansion reactions.

Results and Discussion

Syntheses and Characterization of $(\eta^2\text{-TCNE})\text{M}(\eta\text{-CNC}_6\text{H}_3\text{-2,6-Me}_2)_2$ [M = Pt (1**), Pd (**2**), Ni (**3**)].** Christofides and co-workers reported the synthesis of $(\eta^2\text{-TCNE})\text{Pt}(\eta\text{-CNC}_6\text{H}_3\text{-2,6-Me}_2)_2$ (**1**) by treatment of $[\text{Pt}_3(\text{CNC}_6\text{H}_3\text{-2,6-Me}_2)_6]$ with TCNE. Characterization of the product was performed by ¹H and ¹³C NMR, IR, and elemental analysis.¹⁸ Nickel and palladium analogues of this Pt complex, $(\eta^2\text{-TCNE})\text{Ni}(\eta\text{-CN}^i\text{Bu})_2$, $(\eta^2\text{-TCNE})\text{Pd}(\eta\text{-CN}^i\text{Bu})_2$, and $(\eta^2\text{-TCNE})\text{Pd}(\eta\text{-CNC}_6\text{H}_5)_2$, were synthesized by treatment of ill-characterized “ $\text{M}(\text{CNR})_2$ ” with TCNE.¹⁹ These complexes were also characterized by spectroscopic methods, and the molecular structure of $(\eta^2\text{-TCNE})\text{Ni}(\eta\text{-$

(17) Yamazaki, H.; Aoki, K.; Yamamoto, Y.; Wakatsuki, Y. *J. Am. Chem. Soc.* **1975**, *97*, 3546.

(18) Christofides, A. *J. Organomet. Chem.* **1983**, *259*, 355.

(19) (a) Otsuka, S.; Nakamura, A.; Tatsuno, Y. *J. Am. Chem. Soc.* **1969**, *91*, 6994. (b) Otsuka, S.; Yoshida, T.; Tatsuno, Y. *J. Am. Chem. Soc.* **1971**, *93*, 6462. (c) Ittel, S. D. *Inorg. Chem.* **1977**, *16*, 2589.

Table 1. ^1H NMR, ^{13}C NMR, and IR Spectral Data of **1**, **2**, and **3** in CDCl_3

		1	2	3
^1H NMR (600 MHz)	Me	2.52 (s, 12H, Me)	2.51 (s, 12H)	2.50 (s, 12H),
	H _{meta}	7.23 (d, 4H, $J = 7.7$ Hz)	7.21 (d, 4H, $J = 7.7$ Hz)	7.16 (d, 4H, $J = 7.7$ Hz)
	H _{para}	7.36 (t, 2H, $J = 7.7$ Hz)	7.34 (t, 2H, $J = 7.7$ Hz)	7.28 (t, 2H, $J = 7.7$ Hz)
^{13}C NMR (150 MHz)	Me	18.5	18.5	18.8
	CCN	13.6 ($^1J_{\text{C-Pt}} = 295$ Hz)	21.1	18.4
	CNC ₆ H ₃ Me ₂	125.1, 128.4, 130.9, 135.7	125.1, 128.2, 130.6, 135.6	126.9, 128.1, 129.4, 135.3
		112.5 ($^2J_{\text{C-Pt}} = 59$ Hz)	112.1	115.5
IR (KBr) (cm^{-1})	CCN	159.4	146.8	156.3
	CNC ₆ H ₃ Me ₂	2227	2227	2224
	(NC) ₂ C	2187, 2176	2198, 2178	2169, 2147

Table 2. ^{13}C – ^{195}Pt Coupling Constant of Complex **1** and Other Platinum–Alkene Complexes

complex	δ C _{alkene}	$^1J_{\text{C-Pt}}$ (Hz)	δ C _{CN}	$^3J_{\text{C-Pt}}$ (Hz)	ref
$\text{K}^+[\text{PtCl}_3(\text{C}_2\text{H}_4)]^-$ ^a	67.1	195 ± 2			21
$(\text{PPh}_3)_2\text{Pt}(\text{C}_2\text{H}_4)$ ^a	39.6	194 ± 2			21
$(\text{PPh}_3)_2\text{Pt}[\text{Ph}(\text{H})\text{C}=\text{C}(\text{CN})_2]$ ^a	16.2 (59.8) ^c	184 (250)	117.6	55	22
$(\eta^2\text{-TCNE})\text{Pt}(\eta\text{-CNC}_6\text{H}_3\text{-2,6-Me}_2)_2$ (1) ^b	13.6	295	112.5	59	this work

^a In CD_2Cl_2 . ^b In CDCl_3 . ^c Figures in parentheses are the chemical shift and the coupling constant of the carbon due to $\text{Ph}(\text{H})\text{C}=\text{C}(\text{CN})_2$.

Table 3. Bond Lengths of Alkene and α Angles of Uncoordinated and Coordinated Alkenes

compound	C–C(alkene), Å	$\Delta(\text{C}–\text{C})$, ^a Å	α , ^b deg.	ref
C_2H_4 ^c	1.337(2)	0	0	8
$\text{K}[(\text{C}_2\text{H}_4)\text{PtCl}_3] \cdot \text{H}_2\text{O}$ ^d	1.345(4)	0.038	32.5	7
TCNE ^e	1.344(3)	0	0	10
$(\eta^2\text{-TCNE})\text{IrBr}(\text{CO})(\text{PPh}_3)_2$ ^e	1.506(15)	0.162	70.4	23
$(\eta^2\text{-TCNE})\text{Ir}(\text{CO})(\text{C}_6\text{N}_4\text{H})(\text{PPh}_3)_2$ ^e	1.526(12)	0.182	67.4	24
$(\eta^2\text{-TCNE})\text{Pt}(\kappa\text{-PPh}_3)_2$ ^e	1.494	0.150	63.8	9
$(\eta^2\text{-TCNE})\text{Ni}(\eta\text{-CN}^t\text{Bu})_2$ ^e	1.476(5)	0.132	56.8	20
$(\eta^2\text{-TCNE})\text{Pt}(\eta\text{-CNC}_6\text{H}_3\text{-2,6-Me}_2)_2$ (1) ^e	1.511(5)	0.167	61.0	this work
$(\eta^2\text{-TCNE})\text{Pd}(\eta\text{-CNC}_6\text{H}_3\text{-2,6-Me}_2)_2$ (2) ^e	1.479(3)	0.135	53.1	this work
$(\eta^2\text{-TCNE})\text{Ni}(\eta\text{-CNC}_6\text{H}_3\text{-2,6-Me}_2)_2$ (3) ^e	1.478(4)	0.134	54.5	this work

^a $\Delta(\text{C}–\text{C})$ is the difference in the C–C distance between the complexed and uncomplexed forms of the alkene ligand. ^b α is the angle defined by Figure 3 (see ref 20). ^c Determined by electron diffraction. ^d Determined by neutron diffraction. ^e Determined by X-ray diffraction.

Table 4. Representative Bond Lengths, Angles, and Torsion Angles for **1**, **2**, and **3**

	Pt (1)	Pd (2)	Ni (3)
M1–C1	1.967(3)	2.016(2)	1.867(2)
M1–C10	1.965(3)	2.017(2)	1.868(3)
C1–N1	1.148(4)	1.146(3)	1.155(3)
C10–N2	1.149(5)	1.147(2)	1.155(3)
M1–C19	2.081(3)	2.088(2)	1.968(2)
M1–C20	2.068(3)	2.066(2)	1.968(2)
C19–C20	1.511(5)	1.479(3)	1.478(4)
C1–M–C10	97.21(15)	99.22(9)	101.94(11)
C19–M–C20	42.71(14)	41.72(9)	44.13(11)
C21–C19–C22	114.4(3)	114.69(19)	116.1(2)
C23–C20–C24	115.2(3)	115.2(2)	114.5(2)
C21–C19–C20–C24	–145.4(3)	–150.2(2)	146.3(2)
C22–C19–C20–C23	142.6(3)	146.2(2)	–149.0(2)

CN^tBu)₂ was determined by crystallography.²⁰ In this project, we synthesized platinum, palladium, and nickel complexes bearing a η^2 -TCNE and two η -CNC₆H₃-2,6-Me₂ ligands, $(\eta^2\text{-TCNE})\text{Pt}(\eta\text{-CNC}_6\text{H}_3\text{-2,6-Me}_2)_2$ (**1**), $(\eta^2\text{-TCNE})\text{Pd}(\eta\text{-CNC}_6\text{H}_3\text{-2,6-Me}_2)_2$ (**2**), and $(\eta^2\text{-TCNE})\text{Ni}(\eta\text{-CNC}_6\text{H}_3\text{-2,6-Me}_2)_2$ (**3**), by the reaction of TCNE with “M(CNC₆H₃-2,6-Me₂)₂” [M = Pt, Pd, Ni] *in situ* generated from Pt(cod)₂, Pd₂(dba)₃·CHCl₃, or Ni(cod)₂ with 2 equiv of CNC₆H₃-2,6-Me₂ in ether at room temperature for 2 h. Addition of TCNE to an ethereal homo-

geneous solution of “M(CNC₆H₃-2,6-Me₂)₂” resulted in instant formation of insoluble materials, of which spectroscopic data in CDCl_3 showed the formation of the desired $(\eta^2\text{-TCNE})\text{M}(\eta\text{-CNC}_6\text{H}_3\text{-2,6-Me}_2)_2$ in 58–94% yields (Scheme 3). Spectral data (^1H and ^{13}C NMR in CDCl_3 and IR in KBr) of the complexes, **1**, **2**, and **3** are summarized in Table 1. All of these three complexes showed ^1H resonances consisting of a single set of signals due to the methyl protons and the para and meta protons, which appeared as a singlet (δ 2.50–2.52), doublet (δ 7.16–7.23), and a triplet (δ 7.28–7.36). This is consistent with the fact that these complexes have two magnetically equivalent CNC₆H₃-2,6-Me₂ ligands. ^{13}C NMR spectra of **1**, **2**, and **3** also suggest the existence of two magnetically equivalent CNC₆H₃-2,6-Me₂ groups. It should be noted that the ^{13}C resonance due to the coordinated carbons of TCNE are seen at δ 18.4, 21.1, and 13.6, which are significantly more upfield than the uncoordinated TCNE (δ 80.3). The ^{13}C – ^{195}Pt coupling constant of **1** is 295 Hz, which is higher than the other known data of platinum–alkene complexes, as shown in Table 2, suggesting stronger Pt–C spin–spin interaction. The most significant upfield shift of the ^{13}C signal of the platinum complex among **1**, **2**, and **3**, as well as the larger ^{13}C – ^{195}Pt coupling constant of **1**, indicates significant contribution of the platinumacyclopropane extreme.

X-ray structure determination of the TCNE complexes **1**–**3** showed the three coordinated planar structures of $(\eta^2\text{-TCNE})\text{M}(\eta\text{-CNC}_6\text{H}_3\text{-2,6-Me}_2)_2$ as expected. As a representative of the three complexes, the ORTEP drawing of the platinum complex is illustrated in Figure 2, and representative bond lengths, angles, and torsion angles are summarized in Table 4. The TCNE ligand is bonded to the platinum center with Pt–C distances of 2.081–(3) and 2.068(3) Å, whereas the two isocyanide ligands are

(20) Stalick, J. K.; Ibers, J. A. *J. Am. Chem. Soc.* **1970**, *92*, 5333.

(21) Chisholm, M. H.; Clark, H. C.; Manzer, L. E.; Stothers, J. B. *J. Am. Chem. Soc.* **1972**, *94*, 5087.

(22) Asaro, F.; Lenarda, M.; Pellizer, G.; Storaro, L. *Spectrochim. Acta, Part A* **2000**, *56*, 2167.

(23) (a) McGinnety, J. A.; Ibers, J. A. *Chem. Commun.* **1968**, *5*, 235. (b) Manojlovic-Muir, L.; Muir, K. W.; Ibers, J. A. *Discuss. Faraday Soc.* **1969**, *47*, 84.

(24) Ricci, J. S.; Ibers, J. A. *J. Am. Chem. Soc.* **1971**, *93*, 2391.

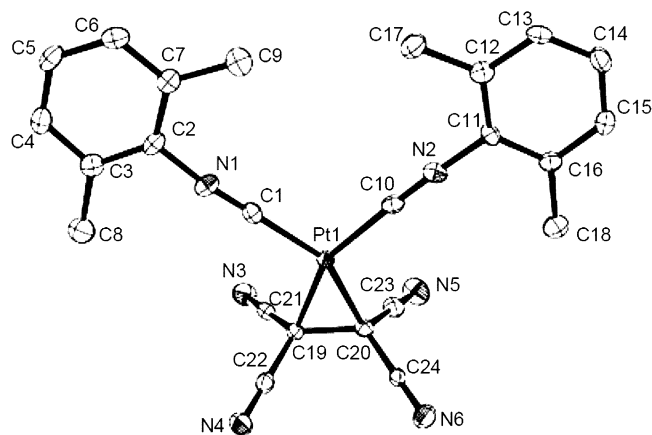


Figure 2. Molecular structure of **1** in the crystal. Ellipsoids represent 50% probability; hydrogen atoms are omitted for clarity.

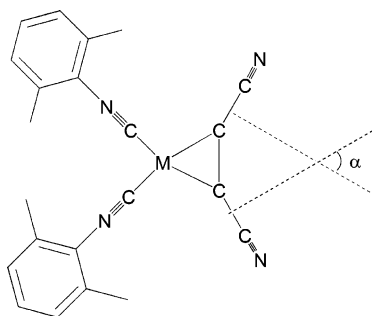
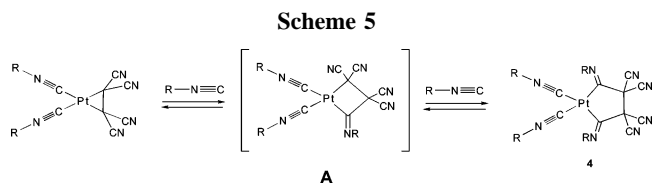
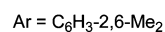
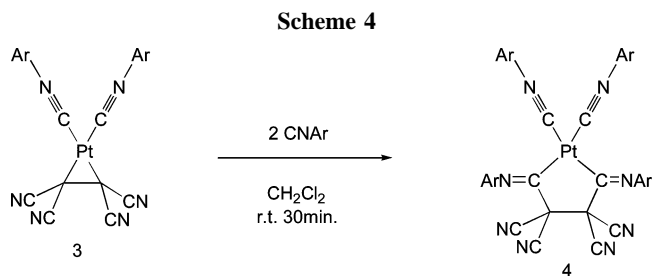


Figure 3. Definition of the angle α (deg).



bound to the platinum with Pt–C distances of 1.967(3) and 1.965(3) Å. The carbon–carbon distance of the coordinated C=C moiety is 1.511 Å, which is significantly longer than that of the TCNE molecule by 0.17 Å. Four CN groups attached to the central carbons of TCNE are significantly out of plane by the coordination, suggesting a change of their hybridization from sp^2 to sp^3 . Ibers and co-workers proposed the α angle for discussing the deviation of planarity of the alkene by coordination to the transition metal center, as shown in Figure 3.²⁰ The α angle of **1** is 61.0°. The C–C bond distance and the planarity of the coordinated TCNE are important indications of a combination of donation and back-donation; the longer C–C distance and the larger α angle suggest the larger contribution of back-donation, giving a typical metallacyclopropane extreme. Two of the most famous examples of the metallacyclopropane extreme in the literature are (η^2 -TCNE)Pt(κ -PPh₃)₂ and (η^2 -

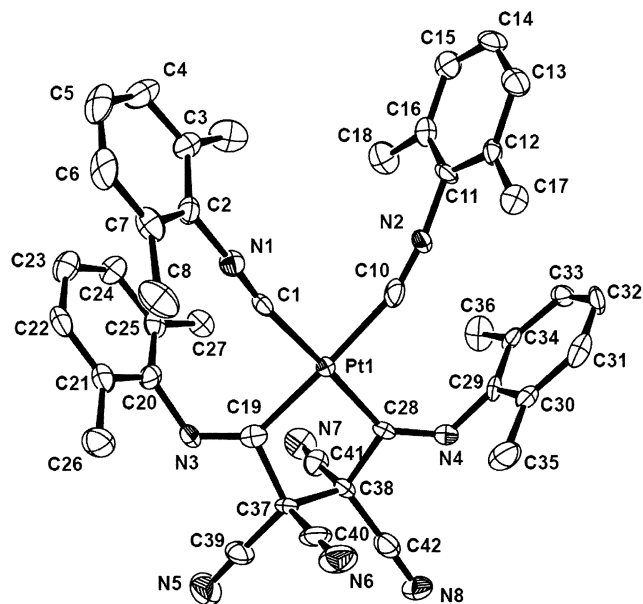
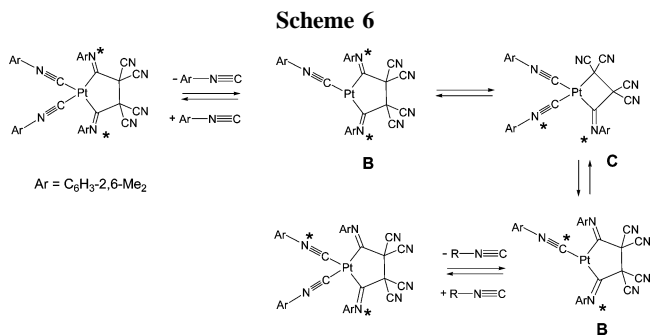


Figure 4. Molecular structure of **4** in the crystal. Ellipsoids represent 50% probability; hydrogen atoms and solvate molecules are omitted for clarity.



TCNE)IrBr(CO)(PPh₃)₂, of which C–C distances are 1.494 and 1.506(15) Å, whereas the α angles are 63.8 and 70.4°, respectively. The C–C distance of 1.511(5) Å of **1** is slightly longer than the above two typical metallacyclopropane extremes, but the α angle of 61.0° is somewhat smaller. However, these apparently differ from those of Zeise's salt (C–C = 1.375(4) Å, α angle = 32.5°), which is known as a typical π -complex extreme, indicating that the coordination mode of TCNE to the platinum is a platinacyclopropane extreme. The C–C distances and the planarity of the coordinated TCNE in the Pd and Ni homologues of **1** are shown in Table 3. The features are less significant than in **1**; back-donation favorably contributes to the coordination of TCNE in the nickel and palladium homologues, too [Ni (**3**): C–C = 1.478(4) Å, α angle = 54.5°; Pd (**2**): C–C = 1.479(3) Å, α angle = 53.1°].

Reaction of Complexes 1, 2, and 3 with 2 equiv of CNC₆H₃-2,6-Me₂. The molecular structures of **1–3** indicate that these complexes have structures that can be considered to be the metallacyclopropane extreme. In particular, the C–C bond length of the coordinated TCNE is the longest among the TCNE–transition metal complexes listed in the Cambridge Data Base. These results prompted us to examine the reaction of **1–3** with CNC₆H₃-2,6-Me₂ to look at the possibility of insertion of CNC₆H₃-2,6-Me₂ into the metal–carbon bond of the metallacyclopropane. ¹H NMR observation of the treatment of **1** with CNC₆H₃-2,6-Me₂ in CH₂Cl₂ at room temperature resulted in consumption of 2 equiv of CNC₆H₃-2,6-Me₂ to form the new complex **4** quantitatively; chromatographic purification of the

Table 5. Representative Bond Lengths, Angles, and Torsion Angles for the Complex 4

Pt1–C1	2.008(7) [2.002(8)]	Pt1–C10	1.998(9) [2.007(10)]
Pt1–C19	2.028(8) [2.040(8)]	Pt1–C28	2.017(6) [2.043(7)]
C1–N1	1.149(9) [1.154(10)]	C10–N2	1.151(12) [1.144(13)]
C19–N3	1.271(10) [1.263(12)]	C28–N4	1.283(10) [1.248(10)]
C19–C37	1.581(11) [1.583(10)]	C37–C38	1.535(13) [1.577(14)]
C38–C28	1.583(11) [1.555(11)]	C1–Pt1–C10	85.3(3) [87.4(3)]
C19–Pt1–C28	83.2(3) [82.0(3)]	C19–N3–C20	121.3(7) [123.5(7)]
C28–N4–C29	123.2(6) [119.5(6)]	C39–C37–C40	109.3(8) [110.2(7)]
C19–C37–C40	106.8(6) [111.6(6)]	C41–C38–C42	108.9(6) [109.7(6)]
C28–C38–C41	108.8(8) [109.0(6)]	C19–C37–C38–C28	48.1(8) [–43.7(6)]
C39–C37–C38–C42	–64.2(9) [–50.7(7)]	C39–C37–C38–C41	56.3(10) [–171.6(6)]
C40–C37–C38–C41	177.9(6) [–50.2(8)]	C40–C37–C38–C42	57.4(8) [70.7(7)]

Table 6. Crystallographic Data for 1, 2, 3, and 4

	1	2	3	4
empirical formula	C ₂₄ H ₁₈ N ₆ Pt	C ₂₄ H ₁₈ N ₆ Pd	C ₂₄ H ₁₈ N ₆ Ni	C ₄₃ H ₃₈ N ₈ PtCl ₂
fw	585.54	496.85	449.15	932.83
cryst syst	monoclinic	triclinic	triclinic	monoclinic
lattice type	primitive	primitive	primitive	primitive
a, Å	8.0089(17)	7.9700(13)	7.9194(15)	13.507(2)
b, Å	12.711(3)	12.2700(19)	12.358(2)	43.455(7)
c, Å	21.766(4)	13.2300(19)	12.986(2)	15.453(3)
α, deg	90	60.100(9)	60.307(7)	90
β, deg	93.152(5)	77.100(11)	77.067(8)	114.3223(19)
γ, deg	90	79.420(12)	79.767(9)	90
V, Å ³	2212.5(8)	1089.3(3)	1072.7(3)	8265(2)
space group	P2 ₁ /n	P $\bar{1}$	P $\bar{1}$	P2 ₁ /n
Z value	4	2	2	8
D _{calc} , g/cm ³	1.758	1.515	1.390	1.499
F ₀₀₀	1128.00	500.00	464.00	3712.00
μ(Mo Kα)	63.395	8.756	9.277	35.512
2θ _{max}	55.0	55.0	54.9	55.0
radiation		Mo Kα (λ = 0.71070 Å) graphite monochromated		
R _{int}	0.038	0.028	0.037	0.075
no. of rflns measd	17 337	8897	8741	58 284
no. of unique rflns	4957	4790	4694	18 721
refln/param ratio	16.60	16.04	15.71	18.12
residuals: R (all rflns)	0.0362	0.0293	0.0517	0.0929
residuals: R1 (I > 2.00σ(I))	0.0251	0.0260	0.0405	0.0602
residuals: wR2 (all rflns)	0.0535	0.0768	0.1198	0.1577
goodness of fit indicator	1.002	1.001	1.002	1.002
max. shift/error in final cycle	0.000	0.000	0.000	0.000
max. peak in final diff map, e [–] /Å ³	2.14	0.54	0.69	2.35
min. peak in final diff map, e [–] /Å ³	–1.19	–0.48	–0.37	–2.76

crude sample gave **4** as yellow microcrystals in 68% yield (Scheme 4). Since the formed complex showed dynamic behavior in the NMR spectra in CD₂Cl₂, the assignment of NMR data was carried out at 0 °C. Two magnetically inequivalent aryl signals were seen in the ¹H and ¹³C NMR spectra, indicating the existence of two types of CNC₆H₃-2,6-Me₂ moieties in the molecule. The ¹H resonances due to the meta and para protons of the coordinated CNC₆H₃-2,6-Me₂ group were observed at δ 6.97 and 7.16 in a ratio of 2:1, which have similar chemical shifts to those of **1**. The other two signals due to the other type of CNC₆H₃-2,6-Me₂ were seen at δ 6.18 and 6.70 in a ratio of 1:2. In the ¹³C NMR spectra, 14 signals were observed, which contained three signals with ¹³C–¹⁹⁵Pt coupling respectively [δ 60.8 (²J_{C–Pt} = 235 Hz), 135.7 (¹J_{C–Pt} = 980 Hz), and 173.8 (¹J_{C–Pt} = 1145 Hz), due to C37 (C38), C19 (C28), and C1 (C10) in Figure 4, respectively]. Three IR absorptions were visible at 2198, 1622, and 1591 cm^{–1}; the former is due to the coordinated CNC₆H₃-2,6-Me₂, whereas the latter two resembled the C=N stretching vibration of the imido group.

These features in spectroscopy are consistent with those deduced from the molecular structure of **4**, which has two CNC₆H₃-2,6-Me₂ groups bonded to the platinum center and a platinacyclopentane structure consisting of two carbons of the TCNE and two CNC₆H₃-2,6-Me₂ groups, as shown in Figure 4. The crystal contains two independent but chemically equivalent molecules of **4**. Bond distances and angles of the second

Table 7. Exchange Rate Constants between the Coordinated CNC₆H₃-2,6-Me₂ and the Imido group CNC₆H₃-2,6-Me₂ in **4 Measured by SST at –10, –20, and –30 °C (k; s^{–1})**

complex	–10 °C	–20 °C	–30 °C
4	1.72	0.66	0.23
4 + 10 equiv of CNAr	0.21	0.07	0.04

molecule are given in brackets in Table 5. The platinacyclopentane structure was formed by insertion of CNC₆H₃-2,6-Me₂ molecules into each Pt–C bond of the platinacyclopentane extreme of **1**. In contrast to the result that the coordinated CNC₆H₃-2,6-Me₂ groups in **4** have usual C–N and Pt–C bond distances typically seen in isocyanide complexes of platinum,²⁵ the CNC₆H₃-2,6-Me₂ groups in the platinacyclopentane resemble the imido platinum species, of which C–N and Pt–C distances are 1.271(10) [1.263(12)], 1.283(10) [1.248(10)] and 2.028(8) [2.040(8)], 2.017(6) [2.043(7)] Å, respectively. The platinacyclopentane structure is envelope-shaped with two sp²-hybridized carbons derived from the CNC₆H₃-2,6-Me₂ and two sp³ carbons originated from the TCNE.

(25) (a) Kim, Y.-J.; Choi, E.-H.; Lee, S. W. *Organometallics* **2003**, *22*, 3316. (b) Lu, Z.-L.; Mayr, A.; Cheung, K.-K. *Inorg. Chim. Acta* **1999**, *284*, 205. (c) Kemmitt, R. D. W.; McKenna, P.; Russell, D. R.; Prouse, L. J. *J. Chem. Soc., Dalton Trans.* **1989**, 345. (d) Dryden, N. H.; Puddephatt, R. J.; Roy, S.; Vittal, J. J. *Acta Crystallogr. Sect. C: Cryst. Struct. Commun.* **1994**, *50*, 533. (e) Yamada, T.; Tanabe, M.; Osakada, K.; Kim, Y.-J. *Organometallics* **2004**, *23*, 4771.

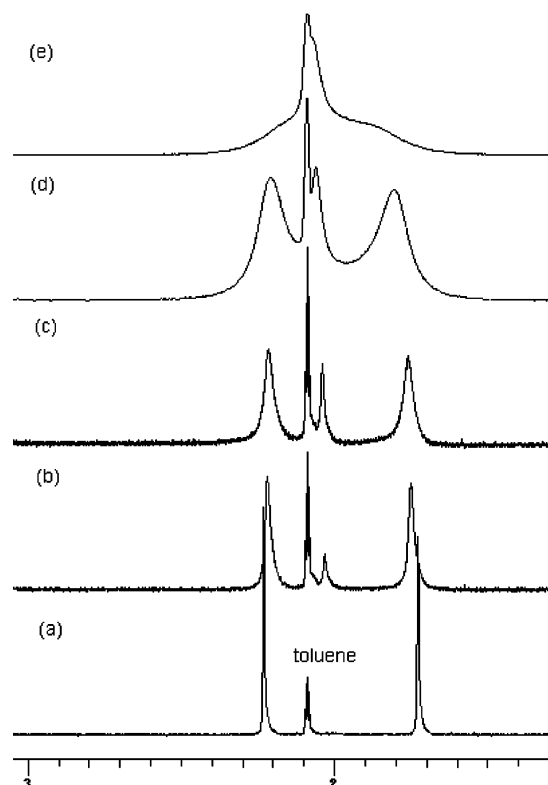


Figure 5. Line shape analysis of complex **4** in toluene- d_8 (a) at 0 °C, (b) at 30 °C, (c) at 40 °C, (d) at 60 °C, and (e) at 77 °C (coalesced).

Solution Dynamics of the Platinacyclopentane. As described above, complex **4** showed dynamic behavior in the solution-state NMR spectra. Variable-temperature ^1H NMR studies²⁶ in toluene- d_8 showed sharp signals due to the two magnetically inequivalent $\text{CNC}_6\text{H}_3\text{-2,6-Me}_2$ groups observed at 0 °C, as described above. All of the ^1H resonances were broadened on raising the temperature. As shown in Figure 5, the methyl signals at δ 1.73 and 2.23 due to the inequivalent $\text{CNC}_6\text{H}_3\text{-2,6-Me}_2$ coalesced at 77 °C; this indicates the exchange of two magnetically inequivalent $\text{CNC}_6\text{H}_3\text{-2,6-Me}_2$ moieties in the molecule. Thus, the exchange rate was supplied for 671 s^{-1} , from which ΔG^\ddagger_{350} at coalescence temperature is calculated to be 16 ± 1 kcal/mol. The exchange rate was alternatively estimated from the spin-saturation transfer measurement²⁷ in CD_2Cl_2 at -30 , -20 , -10 , and 0 °C (Figure 6). Irradiation of the signal at δ 6.18 due to the para-proton of the imidoyl $\text{CNC}_6\text{H}_3\text{-2,6-Me}_2$ resulted in a decrease of the peak intensity of the signal at δ 7.16 due to the para-proton of the coordinated $\text{CNC}_6\text{H}_3\text{-2,6-Me}_2$. The estimated ΔG^\ddagger_{350} is 16 ± 1 kcal/mol, which is similar to that estimated from the line shape analysis described above. These data clearly demonstrated the exchange process between the coordinated $\text{CNC}_6\text{H}_3\text{-2,6-Me}_2$ and the imidoyl $\text{CNC}_6\text{H}_3\text{-2,6-Me}_2$ in **4**, which must involve the cleavage process of the C–C bond in the platinacyclopentane. Interestingly, the exchange of two $\text{CNC}_6\text{H}_3\text{-2,6-Me}_2$ moieties was

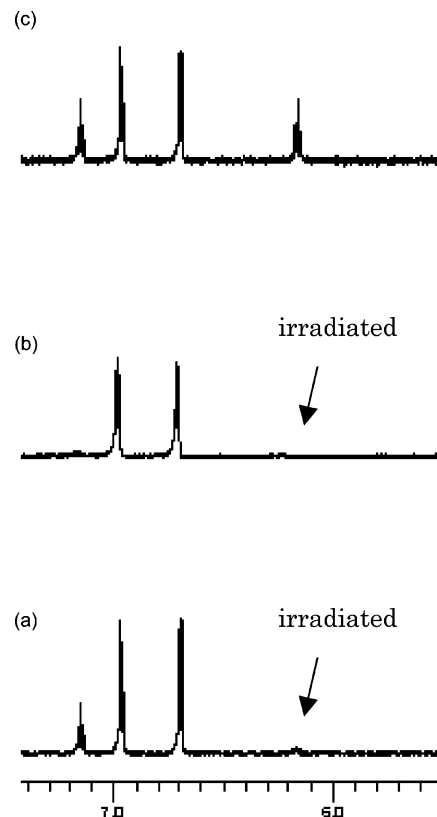


Figure 6. Spin-saturation transfer measurement of complex **4** in CD_2Cl_2 : (a) spectrum with irradiation of the signal appearing as a triplet at δ 6.18 at -30 °C, (b) spectrum with irradiation of the signal appearing as a triplet at δ 6.18 at 0 °C, (c) spectrum with no irradiation at rt.

slower in the presence of 10 equiv of $\text{CNC}_6\text{H}_3\text{-2,6-Me}_2$. As shown in Table 7, the rate constants estimated by the spin-saturation transfer measurements at -30 to -10 °C are increased by raising the temperature in either the presence or absence of $\text{CNC}_6\text{H}_3\text{-2,6-Me}_2$. In this temperature range, the exchange rate constants (k) in the presence of 10 equiv of $\text{CNC}_6\text{H}_3\text{-2,6-Me}_2$ are 1 order of magnitude smaller than those in its absence.

Mechanistic Considerations. As described above, reaction of the platinum complex **1** with 2 equiv of $\text{CNC}_6\text{H}_3\text{-2,6-Me}_2$ resulted in formation of the complex **4**. Crystallographic studies revealed that **1** is a platinacyclopropane extreme, whereas **4** has a platinacyclopentane structure. Consequently, the reaction from **1** to **4** can be considered as a ring expansion of the three-membered platinacycle to the five-membered complex by incorporation of two molecules of $\text{CNC}_6\text{H}_3\text{-2,6-Me}_2$. A plausible mechanism is illustrated in Scheme 5, in which two $\text{CNC}_6\text{H}_3\text{-2,6-Me}_2$ are inserted into two Pt–C bonds in **1** stepwise. Although attempted spectroscopic detection was not successful, a platinacyclobutane **A** is possibly involved as an intermediate of this scheme. Analogous stepwise insertion of two CNR is proposed in the reaction of a cobalt–alkyne complex with CNR reported by Yamazaki and co-workers (Scheme 2), where both the cobaltacyclobutene and cobaltacyclopentene complexes were isolated and characterized by crystallography.¹⁷ Since the cobalt–alkyne complex can be considered as a cobaltacyclopentene, the mechanism proposed for the cobalt–alkyne complex is a good support for the stepwise insertion of the platinacyclopropane to platinacyclopentane via the platinacyclobutane. The fluxional behavior of **4** in the presence or absence of excess $\text{CNC}_6\text{H}_3\text{-2,6-Me}_2$ revealed the exchange processes between the imidoyl $\text{CNC}_6\text{H}_3\text{-2,6-Me}_2$ and the coordinated

(26) (a) Crabtree, R. H., Ed. *The Organometallic Chemistry of the Transition Metals*, 4th ed.; Wiley: New York, 2001; Chapter 10, p 284. (b) Oki, M. *Applications of Dynamic NMR Spectroscopy to Organic Chemistry*; VCH: Deerfield Beach, FL, 1985; Chapter 1, p 11.

(27) (a) Faller, J. W. *Determination of Organic Structures by Physical Methods*; Nachod, F. C., Zuckerman, J. J., Eds.; Academic Press: New York, 1973, Vol. 5, Chapter 2. (b) Sandstrom, J. *Dynamic NMR Spectroscopy*; Academic Press: New York, 1982. (c) Derome, A. E. *Modern NMR Techniques for Chemistry Research*; Pergamon: Oxford, 1987. (d) Jarek, R. L.; Flesher, R. J.; Shin, S. K. *J. Chem. Educ.* **1997**, *74*, 978.

CNC₆H₃-2,6-Me₂. A reasonable interpretation for the retardation of the exchange rate between the imidoyl CNC₆H₃-2,6-Me₂ and the coordinated CNC₆H₃-2,6-Me₂ is that the reaction is triggered by dissociation of CNC₆H₃-2,6-Me₂ from **4**, as shown in Scheme 6. The dissociation produces a coordinatively unsaturated species **B**, on which degradation of the platinacyclopentane reversibly forms the platinacyclobutane intermediate **C** via deinsertion of CNC₆H₃-2,6-Me₂. The interconversion between the platinacyclopentane and the platinacyclobutane via **B** explains the solution dynamics suggesting the exchange of the imidoyl CNC₆H₃-2,6-Me₂ and coordinated CNC₆H₃-2,6-Me₂. Thus, all of the results described in the solution dynamics in this paper by association with the CNC₆H₃-2,6-Me₂ exchange processes are summarized in Scheme 6.

An interesting question that has not been solved in our experiments is why only the platinum–TCNE complex can react with CNC₆H₃-2,6-Me₂, and the palladium and nickel homologues do not. The molecular structures of **2** and **3** described above suggest that they are also considered to be metallacyclopropane extremes from the C=C bond distance (1.478(4), 1.479(3) Å) and the α -angles (54.5, 53.1°), although contribution of back-donation in the nickel and palladium complexes is smaller than that of the platinum homologues. Two possibilities can be proposed; one is a kinetic reason, in which the insertion of CNC₆H₃-2,6-Me₂ requires the highest contribution of back-donation, and only the platinum complex is adopted in this criterion. Another is a thermodynamic explanation, in which the insertion of CNC₆H₃-2,6-Me₂ also takes place in the nickel and palladium homologues, but it is essentially reversible. In this case, the equilibrium is favored for the metallacyclopropane for nickel and palladium, whereas platinum is favored for the metallacyclopentane. Further investigation with assistance of theoretical studies is awaited for discussion.

Conclusion

As described above, we have reported the first example of ring expansion of a metallacyclopropane to a metallacyclopentane by insertion of isocyanides, in which both of the molecular structures are unequivocally determined by crystallography. Among the three complexes with homologous structures, (η^2 -TCNE)M(η -CNC₆H₃-2,6-Me₂)₂ (M = Ni, Pd, Pt), only the platinum complex is reactive toward ring expansion. The solution dynamics of the platinacyclopentane showed the exchange of the imidoyl CNC₆H₃-2,6-Me₂ and the coordinated CNC₆H₃-2,6-Me₂, suggesting the insertion of CNC₆H₃-2,6-Me₂ to be reversible. A dissociative mechanism is proposed. As described in the Introduction, coordination of alkenes is generally explained by the Dewar–Chatt–Dunkanson model, and (η^2 -TCNE)Pt(κ -PPh₃)₂ is one of the most famous examples of a “metallacyclopropane extreme”, in which back-donation from the metal to the C=C bond is the primary factor for the coordination. Since the metal–carbon bond is reactive with various unsaturated molecules, it is probable that ring expansion from metallacyclopropane to metallacyclobutane by insertion of CO or CNR and to metallacyclopentane by alkene generally occurs in organometallic reactions. They are indeed proposed in the mechanisms of catalytic reactions. Nevertheless, little has been reported on the ring expansion with unequivocal evidence, including the molecular structures of the starting material and the product. To our best knowledge, the present paper is the first investigation of the ring expansion from metallacyclopropane to metallacyclopentane with unequivocal evidence on the molecular structures, providing new and important aspects for the understanding of the reactions of coordinated alkenes.

Further mechanistic studies as well as the reactions of metallacycles synthesized in this paper are in progress.

Experimental Section

General Procedures. All experiments were carried out under an argon atmosphere using standard Schlenk techniques. All solvents were distilled over appropriate drying reagents prior to use (toluene, hexane, Et₂O; Ph₂CO/Na, CH₂Cl₂; CaH₂). The ¹H NMR spectra were taken with a JEOL ECA 600 spectrometer. Chemical shifts were recorded in ppm from the internal standard (¹H, ¹³C: solvent). IR spectra were recorded in cm⁻¹ on a JASCO FT/IR-550 spectrometer. Melting points were measured on a Yanaco SMP3 micro melting point apparatus. HRMS spectrum was recorded on a JEOL Mstation JMS-70 apparatus. Elemental analyses were performed by the Elemental Analysis Center, Faculty of Science, Kyushu University. Starting materials Ni(cod)₂,²⁸ Pd₂(dba)₃·CHCl₃,²⁹ and Pt(cod)₂³⁰ were synthesized by the method reported in the literature.

Preparation of the Metallacyclopropanes. (η^2 -TCNE)Pt(η -CNC₆H₃-2,6-Me₂)₂ (**1**). In a 20 mL Schlenk tube, Pt(cod)₂ (200 mg, 0.49 mmol) and CNC₆H₃-2,6-Me₂ (128 mg, 0.98 mmol) were dissolved in Et₂O (30 mL) at room temperature and stirred for 1 h. The resulting solution was filtered by passing the mixture through a short pad of Celite. To the filtrate was added tetracyanoethylene (62 mg, 0.49 mmol), and the mixture was stirred for 2 h at room temperature. The resulting pale yellow precipitate was washed with Et₂O and dried *in vacuo*, affording **1** in 58% yield (166 mg). Further purification by recrystallization from toluene gave a pale yellow block, mp 149 °C (dec). IR: $\nu_{\text{C}\equiv\text{N}}$ 2227, 2187, 2176 cm⁻¹. ¹H NMR (600 MHz, CDCl₃, rt): δ 2.52 (s, 12H, Me), 7.23 (d, 4H, H_{meta}, J = 7.7 Hz), 7.36 (t, 2H, H_{para}, J = 7.7 Hz). ¹³C NMR (150 MHz, CDCl₃, rt): δ 13.6 (¹J_{C–Pt} = 295 Hz), 18.5 (Me), 112.5 (²J_{C–Pt} = 59 Hz), 125.1, 128.4, 130.9, 135.7, 159.4. HRMS: calcd for ¹²C_{24¹H₁₈¹⁴N₆¹⁹⁵Pt 586.1319; found 586.1322.}

(η^2 -TCNE)Pd(η -CNC₆H₃-2,6-Me₂)₂ (**2**). In a 20 mL Schlenk tube, Pd₂(dba)₃·CHCl₃ (61 mg, 0.059 mmol) and CNC₆H₃-2,6-Me₂ (30 mg, 0.23 mmol) were dissolved in Et₂O (20 mL) at –76 °C. The resulting solution was warmed to 1 °C and stirred for 2 h. After the solution was warmed to room temperature, tetracyanoethylene (15 mg, 0.36 mmol) was added, and the mixture was stirred for 2 h. The yellow solution was removed via syringe and washed with Et₂O, and the resulting green precipitate was dissolved in dichloromethane (20 mL) and filtered by passing the mixture through a short pad of Celite. Concentration of the resulting solution *in vacuo* afforded **2** in 94% yield (56 mg) as a green powder. Further purification by recrystallization from toluene gave the desired complex **2** as a green block, mp 206 °C (dec). IR: $\nu_{\text{C}\equiv\text{N}}$ 2227, 2198, 2178 cm⁻¹. ¹H NMR (600 MHz, CDCl₃, rt): δ 2.51 (s, 12H), 7.21 (d, 4H, H_{meta}, J = 7.7 Hz), 7.34 (t, 2H, H_{para}, J = 7.7 Hz). ¹³C NMR (150 MHz, CDCl₃, rt): δ 18.5 (Me), 21.1, 112.1, 125.1, 128.2, 130.6, 135.6, 146.8. Anal. Calcd for C₂₄H₁₈N₆Pd: C, 58.02; H, 3.65; N, 16.91. Found: C, 58.11; H, 3.59; N, 16.83.

(η^2 -TCNE)Ni(η -CNC₆H₃-2,6-Me₂)₂ (**3**). In a 50 mL Schlenk tube were placed Ni(cod)₂ (100 mg, 0.36 mmol) and CNC₆H₃-2,6-Me₂ (95 mg, 0.72 mmol), and then Et₂O (20 mL) was added at –75 °C. The resulting solution was warmed to –3 °C and stirred for 2 h. Then the color of the solution changed from yellow to dark brown. After the solution was warmed to room temperature, tetracyanoethylene (47 mg, 0.36 mmol) was added, and the mixture was stirred for 2 h. The solution was removed via syringe and washed with Et₂O, and the resulting dark brown precipitate was dissolved in dichloromethane (20 mL) and filtered by passing the

(28) Schunn, R. A. *Inorg. Synth.* **1974**, *15*, 5.

(29) Ukai, T.; Kawazura, H.; Ishii, Y. *J. Organomet. Chem.* **1974**, *65*, 253.

(30) Spencer, J. L. *Inorg. Synth.* **1979**, *12*, 213.

mixture through a short pad of Celite. Concentration of the resulting solution *in vacuo* afforded **3** as a red powder. Purification by recrystallization from toluene or toluene/hexane gave the desired complex **3** in 79% yield (127 mg) as a brown block, mp 210 °C (dec). IR: $\nu_{\text{C}=\text{N}}$ 2224, 2169, 2147 cm^{-1} . ^1H NMR (600 MHz, CDCl_3 , rt): δ 2.50 (s, 12H, Me), 7.16 (d, 4H, H_{meta} , $J = 7.7$ Hz), 7.28 (t, 2H, H_{para} , $J = 7.7$ Hz). ^{13}C NMR (150 MHz, CDCl_3 , rt): δ 18.4, 18.8, 115.5, 126.9, 128.1, 129.4, 135.3, 156.3. Anal. Calcd for $\text{C}_{24}\text{H}_{18}\text{N}_6\text{Ni}$: C, 64.18; H, 4.04; N, 18.71. Found: C, 63.67; H, 4.10; N, 18.55.

Ring Expansion of 1 to (TCNE)Pt(η -CNC₆H₃-2,6-Me₂)₄ (4). In a 5 Φ NMR tube were dissolved **1** (1.00 mg, 1.7 μmol) and naphthalene (internal standard; 1.31 mg, 10 μmol) in CD_2Cl_2 (0.5 mL), to which CNC₆H₃-2,6-Me₂ (0.45 mg, 3.4 μmol) was added. After 1 h, all of **1** disappeared and **4** was formed. Integral values of ^1H resonances due to **4** based on those of naphthalene showed the yield of **1** to be quantitative. The preparative scale experiment is as follows: In a 20 mL Schlenk tube, (η^2 -TCNE)Pt(η -CNC₆H₃-2,6-Me₂)₂ (15 mg, 0.026 mmol) was dissolved in CH_2Cl_2 (3 mL) at room temperature. A CH_2Cl_2 solution (2 mL) of CNC₆H₃-2,6-Me₂ (6.7 mg, 0.051 mmol) was added dropwise over 10 min, and the mixture was stirred for 30 min. The resulting solution was concentrated *in vacuo*, and the residue was purified by column chromatography (silica gel) at -30 °C eluted with CH_2Cl_2 to give (TCNE)Pt(η -CNC₆H₃-2,6-Me₂)₄ in 68% yield as yellow solids (8.1 mg). Further purification by recrystallization from CH_2Cl_2 /hexane gave microcrystals as yellow needles, mp 145 °C (dec). IR: $\nu_{\text{C}=\text{N}}$ 2198, 1622, 1591 cm^{-1} . ^1H NMR (600 MHz, CD_2Cl_2 , 0 °C): δ 2.10 (s, 12H, Me), 2.18 (s, 12H, Me), 6.18 (t, 2H, H_{para} , $J = 7.6$ Hz), 6.70 (d, 4H, H_{meta} , $J = 7.6$ Hz), 6.97 (d, 4H, H_{meta} , $J = 7.6$ Hz), 7.16 (t, 2H, H_{para} , $J = 7.6$ Hz). ^{13}C NMR (150 MHz, CDCl_3): δ 17.8, 18.6, 110.1, 123.9, 125.4, 127.1, 127.4, 129.8, 133.7, 135.7, 150.2, 60.8 ($^2J_{\text{C}-\text{Pt}} = 235$ Hz), 135.7 ($^1J_{\text{C}-\text{Pt}} = 980$ Hz), 173.8 ($^1J_{\text{C}-\text{Pt}} = 1145$ Hz). Anal. Calcd for $\text{C}_{42}\text{H}_{38}\text{N}_6\text{Pt}$: C, 59.50; H, 4.28; N, 13.22. Found: C, 59.42; H, 4.26; N, 13.28.

Variable-Temperature ^1H NMR Studies. Variable-temperature ^1H NMR studies were carried out in a temperature range from 0 to 77 °C. A toluene-*d*₈ solution of **4** was placed in a 5 Φ NMR tube and degassed several times. The tube was sealed in a flame, while the solution was kept in a dry ice/acetone bath in a vacuum. On raising the temperature, all ^1H signals were broadened. Typically, two peaks due to Me groups of inequivalent CNR were coalesced at 77 °C. Thus, the exchange rate at coalescence temperature was calculated according to eq 1,²⁶ and ΔG^\ddagger_{350} was also obtained by the Eyring equation (eq 2).

$$k_c = \frac{\pi}{\sqrt{2}} \Delta\nu \quad (1)$$

where $\Delta\nu$ is the peak separation when the exchange rate is negligibly small and k_c is the rate constant of the exchange at coalescence temperature.

$$\Delta G_c^\ddagger = -RT_c \left[\ln \left(\frac{k_c}{T_c} \right) + \ln \left(\frac{h}{k_B} \right) \right] \quad (2)$$

where ΔG_c^\ddagger is the Gibbs free energy at coalescence temperature, R is the gas constant, T_c is the coalescence temperature, h is the Planck constant, and k_B is the Boltzmann constant.

Spin-Saturation Transfer (SST) Measurement. All SST studies were carried out in a temperature range from -30 to 0 °C. A CD_2Cl_2 solution of the complex was placed in a 5 Φ NMR tube and degassed several times. The tube was sealed in a flame, while the solution was kept in a dry ice/acetone bath in a vacuum. The spin-lattice relaxation times were measured by the inversion recovery method as the average of four measurements. The spin saturation and the transfer of the resulting saturated spin from H_B to H_A were carried out by irradiation of H_B for a period of $>5T_1$, which is

enough to equilibrate the exchange and the spin relaxation before the NMR measurement. The decreased intensity of H_A was calculated by comparison of its integral value with the other peak which was not affected by the SST measurements. The data are reported in Tables S-3-1-2 and S-3-2-2 in the Supporting information. The rate constant k was calculated according to eq 3, and the Eyring plot of k at four different temperatures provided the ΔG^\ddagger_{350} value from thermodynamic parameters using eq 4 and eq 5.

$$k = \frac{1}{T_1(\text{H}_A)} \left(\frac{I_{0(\text{H}_A)}}{I_{\text{r}(\text{H}_A)}} - 1 \right) \quad (3)$$

$$\ln \left(\frac{k}{T} \right) = \ln \left(\frac{k_B}{h} \right) - \frac{\Delta H}{RT} + \frac{\Delta S}{R} \quad (4)$$

$$\Delta G = \Delta H - T\Delta S \quad (5)$$

Crystallographic Studies. Single crystals of **1–3** were grown from toluene/hexane, whereas **4** was isolated from CH_2Cl_2 /hexane. X-ray crystallography was performed on a Rigaku Saturn CCD area detector with graphite-monochromated Mo $K\alpha$ radiation ($\lambda = 0.71070$ Å). The data were collected at 123(1) K using ω scans in the θ range of $3.0^\circ \leq \theta \leq 27.5^\circ$ (**1**), $3.1^\circ \leq \theta \leq 27.5^\circ$ (**2**), $3.1^\circ \leq \theta \leq 27.5^\circ$ (**3**), and $3.0^\circ \leq \theta \leq 27.5^\circ$ (**4**). Data were collected and processed using CrystalClear (Rigaku) on a Pentium computer. The data were corrected for Lorentz and polarization effects. The structure was solved by direct methods³¹ for all complexes and expanded using Fourier techniques.³² The non-hydrogen atoms were refined anisotropically. Hydrogen atoms were refined using the riding model. The final cycle of full-matrix least-squares refinement on F^2 was based on 4957 unique reflections and 298 variable parameters for **1**, 4790 unique reflections and 298 variable parameters for **2**, 4694 unique reflections and 298 variable parameters for **3**, and 18721 unique reflections and 1032 variable parameters for **4**. Neutral atom scattering factors were taken from Cromer and Waber.³³ All calculations were performed using the CrystalStructure^{34,35} crystallographic software package. Details of final refinement are summarized in Table 6, and the numbering scheme employed is shown in Figures 2 and 4, which were drawn with ORTEP with 50% probability ellipsoids. Detailed data as well as the bond distances and angles are shown in the Supporting Information.

Supporting Information Available: Variable-temperature NMR data (**4**), ^1H NMR, ^{13}C NMR, and the spin-saturation transfer measurement data (**4**), details of crystallographic studies (**1**, **2**, **3**, and **4**). This material is available free of charge via the Internet at <http://pubs.acs.org>.

OM0608713

(31) (a) Burla, M. C.; Camalli, M.; Carrozzini, B.; Cascarano, G. L.; Giacovazzo, C.; Polidori, G.; Spagna, R. *SIR2002*; 2003. (b) Altomare, A.; Burla, M.; Camalli, M.; Cascarano, G.; Giacovazzo, C.; Guagliardi, A.; Moliterni, A.; Polidori, G.; Spagna, R. *SIR97. J. Appl. Crystallogr.* **1999**, *32*, 115–119. (c) Altomare, A.; Cascarano, G.; Giacovazzo, C.; Guagliardi, A.; Burla, M.; Polidori, G.; Camalli, M. *SIR92. J. Appl. Crystallogr.* **1994**, *27*, 435.

(32) Beurskens, P. T.; Admiraal, G.; Beurskens, G.; Bosman, W. P.; de Gelder, R.; Israel, R.; Smits, J. M. M. *DIRDIF99, The DIRDIF-99 Program System*; Technical Report of the Crystallography Laboratory; University of Nijmegen: Nijmegen, The Netherlands, 1999.

(33) Cromer, D. T.; Waber, J. T. *International Tables for X-ray Crystallography*; Kynoch Press: Birmingham, U.K., 1974; Vol. 4.

(34) (34) *CrystalStructure 3.7.0*, Crystal Structure Analysis Package; Rigaku and Rigaku/MS: The Woodlands, TX 77381, 2000–2005.

(35) Watkin, D. J.; Prout, C. K.; Carruthers, J. R.; Betteridge, P. W. *CRYSTALS Issue 10*; Chemical Crystallography Laboratory: Oxford, U.K., 1996.